Scale Reduction and Maximum Information Loss of Different Information Categories

Ulrich Wieczorek
Chair for Didactics of Geography, University of Augsburg, Germany

ABSTRACT: Not only are the capabilities of the visual system and automatic systems for analyzing the image categories "density," "contour," and "texture" different, but also the information which these categories contain is different. Knowledge about the value of these information categories allows better estimation of the effectiveness of the application of visual or automatic methods for the interpretation of remote sensing data and a better estimation of errors, if scenes of different spatial or radiometric resolution are compared. It can be shown that the content of information is greater for higher spatial resolution than for higher radiometric resolution.

This value depends on the maximum loss of information, if the scale is reduced. Formulas for the calculation of the degree of this loss are deduced for each information category.

INTRODUCTION

INFORMATION FROM REMOTE SENSING DATA is reduced information because the scale of the recorded objects is reduced. The μ-function is used as a measure for the reduction of the information, but it will be shown that this reduction is quite different for the information categories "density," "contour," and "texture." The great difference of information loss for these three information categories and differences of the capability of the human visual system and automatic systems in perceiving and processing different information categories can be one explanation of differring results for ecological land type maps produced by manual cartographic methods or with the aid of remote sensing data and GIS (Lowell, 1990). We have to take into account some important differences between the human visual system and automatic systems concerning these three information categories:

- *Density.* Density can be better recognized by optoelectronic systems than by the human eye. Processing and mapping of density (especially of MSS data) with the aid of different techniques and algorithms (e.g., Gonzales and Wintz, 1987) is superior to the capability of the human visual system.
- *Contours.* Human beings recognize their environment mainly by shapes perceiving those by contours (Fry and Bartley (1935), cited in Lipkin and Rosenfeld (1970), p. 45). Contours are also important for the visual perception of colors (Gilchrist, 1986). Automatic extraction of contours is no problem. But in recognizing objects by their shape, the visual system is superior to automatic systems. It is able to anticipate images represented by an imagination of events which have never been experienced before. A visual image is "a figurative evocation of objects, relations and the common of classes transferring those into a shape which is concrete and suitable for imitation while allowing a high degree of schematization (for one can have an infinite number of perceptions of the same object, but will imagine only some images)" (Piaget and Inhelder, 1966, p. 424). One must have doubts whether an artificial system will ever be able to anticipate images.
- *Textures.* There are successful computer algorithms for the analysis and the classification of textures (Haralick, 1978; Julesz, 1987). The human visual system can only perceive differences of textures which are ascertainable by statistics of second and lower order, whereas automatic systems can record differences concerning statistics of third and higher order (Julesz, 1987). The visual system, however, is superior in synoptic recognition of connections and relationships between image sections of different textures.

Not only knowledge of the different capabilities of the visual system and automatic systems, but also more exact knowledge of the valency of information categories is necessary for obtaining optimal results in analyzing remote sensing data. For this the loss of information in the case of scale reduction for the three information categories can be a measure. This loss depends on the specific image information. If n pixels $P_1, \ldots, P_n$ are united into one pixel P (i.e., $P_1, \ldots, P_n \rightarrow P$), the maximum loss can be determined by calculating

- all possible permutations and combinations of the density values of $P_1, \ldots, P_n$, if P has a certain density d;
- all possible arrangements of contour lines between $P_1, \ldots, P_n$; and
- all possible permutations and combinations of pattern elements for $P_1, \ldots, P_n$.

These numbers will be calculated only for a one-channel image. For an M-channel scene, we have to multiply each number M-times by itself.

SUITABLE DEFINITIONS FOR THE INFORMATION CATEGORIES "DENSITY," "CONTOUR," AND "TEXTURE"

(1) Density is characterized by an integer number between 0 and sm ($0 < sm \leq 255$).

(2) Contours are line elements caused by density differences between pixels. Visual perception of these differences must be possible. Therefore, "open ended" contour lines (OECL) and "circles with cut" (CWC) (Figure 1) would be impossible in a digitized image with only 64 density levels. This is nearly the number of density levels which the human visual system can distinguish. Thus, a density difference at one of the dotted lines must be visible, if there is a density difference between pixel (1; 1) and pixel (2; 1) in Figures 1a and 1b.

For 128 (respectively 256) density levels, a density difference of less than 2 (respectively less than ≈ 4) steps is not perceptible. Then a contour line can be perceptible for the eye between pixel (1; 1) and pixel (2; 1) but not at any of the dotted lines, if the density difference between these two pixels is not greater than 3 (respectively 9) in Figure 1a and not greater than 7 (respectively 21) in Figure 1b, i.e., OECL and CWC are possible. We must, therefore, consider contour arrangements for which OECL

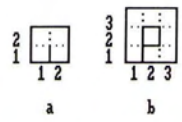

FIG. 1. (a) "Open ended" contour line (OECL) between the pixels (1;1) and (2;1). (b) "Circle with cut" (CWC); cut between the pixels (1;1) and (2;1).

PHOTOGRAMMETRIC ENGINEERING & REMOTE SENSING,
Vol. 58, No. 12, December 1992, pp. 1679–1684.

0099-1112/92/5812–1679$03.00/0

and CWC are allowed and such for which OECL and CWC are not allowed.

(3) Definitions of textures (Wieczorek, 1982, pp. 99–102) call for a certain regularity of the composition of bright and dark pattern elements. We take textures

- as a pattern of black and white pixels ("texture base pattern" (Wieczorek, 1982)), or
- as a pattern of dark and bright "equidensities."

THE CALCULATION OF THE MAXIMUM LOSS OF IMAGE INFORMATION FOR DECREASING IMAGE SCALE

DENSITY

We have $P_1, \ldots, P_n \rightarrow P$. If j is the value of the density sum of the pixels $P_1, \ldots, P_n$, the density value of P is generally the rounded value of j/n.

Permutations of $P_1, \ldots, P_n$ Considered

The calculation concerns the maximum loss of the total image information in the case of scale reduction.

Let $DP_{i,j}$ be the number of permutations $(p(i.j))$ of i density values of which the sum has the value j. If sm is the maximum density value, $DP_{i,j}$ can be calculated by the following recursion ($i = 1, \ldots, n; j = 1, \ldots, n * sm$):

$$DP_{i,j} = DP_{i,j-1} + DP_{i-1,j} - DP_{i-1,j-(sm+1)} \qquad (1)$$

where

$$\begin{aligned} DP_{1,j} &= 1, && \text{if } j \le sm \\ DP_{i,j} &= 0, && \text{if } j \ge sm \\ DP_{i,0} &= 1, && \text{for all values of } i \end{aligned}$$

The validity of Equation 1 is shown with the aid of Figure 2.

Case. $j \le sm$: We obtain the permutations $(p(i.j))$ by adding a new position with the value 0 to the permutations $(p(i\text{-}1.j))$ on the left and by enlarging the value at the first position of permutations $(p(i.j\text{-}1))$ by 1. Therefore, we have $DP_{i,j} = DP_{i,j-1} + DP_{i-1,j}$ (comp. Pascal's triangle).

Case. $j > sm$: All unallowed permutations (surrounded by dotted lines in Figure 2) containing unrealistic density values greater than sm must be deleted. Thus, it follows that when

(1) $i = 1$: $DP_{i,j} = 0$, if $j > sm$.

(2) $i = 2$, $j > sm$: For $j = sm$, only permutations are allowed. If the first value of the $(p(i.j))$ is enlarged, the value "$sm+1$" occurs only on the first position of the $(p(i.j+1))$. The value of the density sum of the other i-1 positions is equal to j-$(sm+1)$. Therefore, we have to delete $DP_{2,j-(sm+1)}$ permutations and to substract $DP_{2,j-(sm+1)}$ from $DP_{2,j-1}$. If all unallowed permutations have been deleted for $j = sm+1$, sm is the greatest value on the first position of the $(p(2.sm+1))$. For $j = sm+2$, we have to delete $DP_{2,j-(2m+1)}$ permutations in the same way as for $j = sm+1$. Continuing in this way, all unallowed permutations can be deleted.

(3) $i > 2$: We presuppose that all unallowed permutations are deleted for i-1 and we apply the same algorithm as for i=2.

Combinations of the Pixels $P_1, \ldots, P_n$ Considered

Most information about contours and textures is not included. There is only the question of the occurrence and the frequency of certain density values. Let $DK_{i,j}$ be the number of combinations $(c(i.j))$ of i density values of which the sum has the value j. We presuppose for the $(c(i.j))$ a monotonous increasing of the density values from left to right. Then $DK_{i,j}$ can be calculated by the following recursion ($i = 1, \ldots, n; j = 1, \ldots, n * sm$):

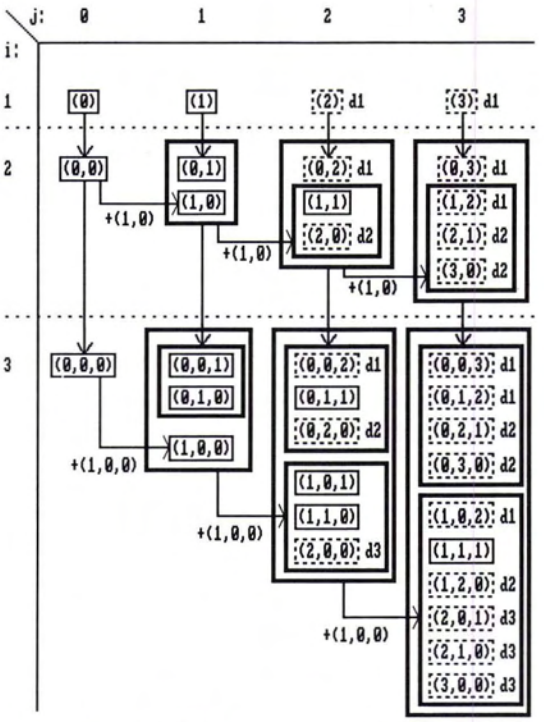

FIG. 2. The permutations $(p(i.j))$ for $i \le 2$ and $j \le 3$, if the maximum density is equal to 1, the $(p(i.j))$ surrounded by perforated lines must be deleted, those surrounded by continuous lines must not be deleted; d_1, d_2, ... means: $(p(i.j))$ is a permutation which is deleted for i = 1, 2, ... or deduced from a per-mutation which has been deleted for i = 1, 2, ...

$$DK_{i,j} = DK_{i-1,j} + DK_{i,j-i} - DK_{i-1,j-i-sm} \qquad (2)$$

where

$$\begin{aligned} DK_{1,j} &= 1, && \text{if } j \le sm \\ DK_{1,j} &= 0, && \text{if } j > sm \\ DK_{i,0} &= 1, && \text{for all values of } i \\ DK_{i,j-i} &= 0, && \text{if } j < i \end{aligned}$$

The validity of Equation 2 is shown with the aid of Figure 3.

Case $j = sm$: We obtain the combinations $(c(i.j))$ by adding a new position with the value 0 to the $(c(i\text{-}1.j))$ on the left and by enlarging each position of the $(c(i.j\text{-}1))$ by 1. Thus, we have (Halder and Heise (1976), p. 78; general theory by Goulden and Jackson (1983), pp. 80–93):

$$DK_{i,j} = DK_{i-1,j} + DK_{i,j-i}$$

Case $j > sm$: All unallowed combinations (surrounded by dotted lines in Figure 3) containing unrealistic density values greater than sm must be deleted. These we delete for $i = 1, 2, \ldots$ in the same way as the unallowed permutations. Thus, $DK_{i-1,j}$ is always a number of allowed combinations and the number of unallowed combinations must be subtracted only from $DK_{i,j-i}$.

Case $j < sm + i$: We have $j\text{-}i < sm$. $j\text{-}i$ is the greatest density value of the combinations $(c(i.j\text{-}i))$. Because of $j\text{-}i+1 \le sm$, no $(c(i.j))$ must be deleted. If $j = sm + i$, we have $j\text{-}i = sm$. After enlarging each position of the $(c(i.j\text{-}i))$ by 1, we have to delete those $(c(i.j))$ containing the density value $sm + 1$ which is the greatest and positioned last. The sum of the values on the first i-1 positions is equal to j-$(sm+1)$. Therefore, the number of the $(c(i.j\text{-}i)) = (c(i.sm))$ with sm in the last position is equal to $DK_{i-1,j-i-sm}$.

Case $j > sm + i$: We presuppose that $DK_{i,j-1}$ is always the

number of the allowed ($c(i.j\text{-}1)$). $DK_{i\text{-}1,j\text{-}i\text{-}sm}$ combinations must be deleted in the same way as for $j = sm+i$.

Total Number of Density Permutations and Density Combinations of $P_1, \ldots, P_n$ for $P_1, \ldots, P_n \rightarrow P$

For the density d of P and the density sum j we have $d - 1/2 \leq j/n = d < + 1/2 \rightarrow d * n - n/2 \leq j \leq d * n + n/2$. If n is an odd number, only the relation "less than" is valid.

(1) Therefore, the number $NP_{s,n,d}$ ($s = sm+1$ = density range) of density permutations for $P_1, \ldots, P_n$ is equal to

$$\sum_{k=n*d-\mathrm{int}(n/2)}^{n*d+\mathrm{int}(n/2)} DP_{n,k} - (DP_{n,n*d-n/2} + DP_{n,n*d+n/2})*t$$

where

$t = 0$, if n is an odd number;
$t = 1/2$, if n is an even number; and
$\mathrm{int}(n/2)$ means the integer function of $n/2$.

If n is an even number and if $j = n*d+n/2$ (resp. $j = n * d\text{-}n/2$), the probability that pixel P has the density d is equal to the probability that pixel P has the density $d+1$ (resp. d-1). Therefore, we can only consider 50 percent of the permutations ($p(i.j)$) for the calculation of $NP_{s,n,d}$. So we must subtract $(DP_{n,n\,.\,s-n/2} + DP_{n,n\,.\,s+n/2})/2$.

(2) We obtain the number $NK_{s,n,d}$ of density combinations for $P_1, \ldots, P_n$ by replacing in Equation 1 $DP_{\ldots}$ by $DK_{\ldots}$.

CONTOURS

Let n pixels $P_1, \ldots, P_n$ be arranged in a rectangle which has a length of m and a width of k pixels. In each line with a length of m pixels there are m-1 vertical line positions (VLP), between two lines there are m horizontal line positions (HLP). The total number of line positions (LP) between all pixels is equal to $m * (k\text{-}1) + (m\text{-}1) * k$.

(1) *OECL allowed:* The number of possibilities for occupying the line positions by a contour line element or by a blank, i.e. by e L/O-occupation, is equal to

$$2^{m*(k-1)+(m-1)*k}$$

(2) *OECL and CWC not allowed:* We calculate the number $K(i,i)$ of all possibilities for occupying the line positions inside a grid net of i by i pixels by L/O in the following way:

Step 1: We begin with two pixel lines, i.e., i=2. We arrange all possible L/O-occupations of VLP between the pixels in line 1 in a line on the top, and those between the pixels in line 2 in a row on the left of a square. Thus, the positions of a 2^{i-1} by 2^{i-1} matrix $\mathbf{M}(i)$, $i=2$, are defined. Into each position (x,y) of the matrix ($\mathbf{M}(i)$ we write all possible L/O-occupations of the HLP (Figure 4A). x marks the rows and y the lines of $\mathbf{M}(i)$.

Step 2: Figure 4 shows how the calculation of $K(2,2)$ can be extended to the calculation of $K(2,3)$ by adding a further pixel in each line. We find all possibilities for occupying the HLP between line 1 and line 2 by L/O in the matrix $\mathbf{M}(i)$, $i=3$.

Step 3: Figure 5 shows how the calculation of the number $h1_{1,x,y}$ of L/O-occupations of the HLP between line 1 and line 2 can be extended from i to $i+1$. We assume that the number $h_{i,x,y}$ has been already calculated for all positions x and y of the matrix $\mathbf{M}(i)$. We reduce $h_{i,x,y}$ in the following way:

$$h_{i,x,y} = h1_{i,x,y} + h0_{i,x,y},$$

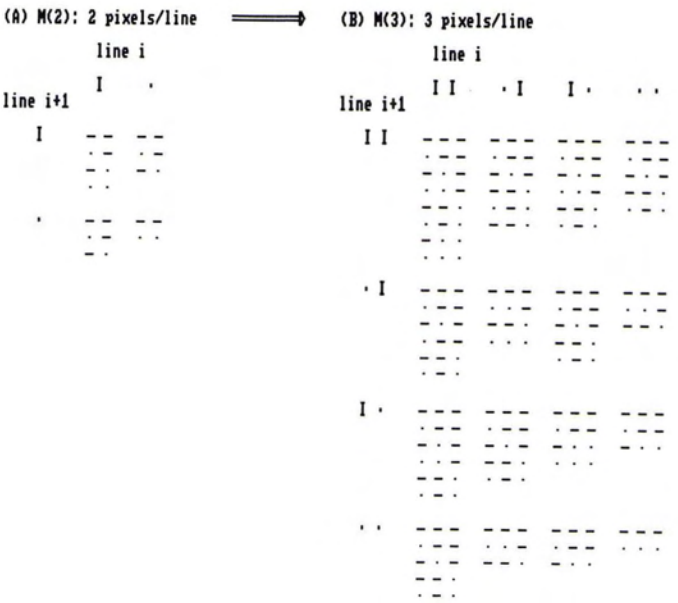

FIG. 4. Two examples of possible occupations of horizontal line positions (HLP) by a contour line element or a blank L/O-occupations) between two pixel lines of different L/O-occupations of vertical line positions (VLP). "I", "-": VLP, HLP occupied: "·": VLP, HLP unoccupied.

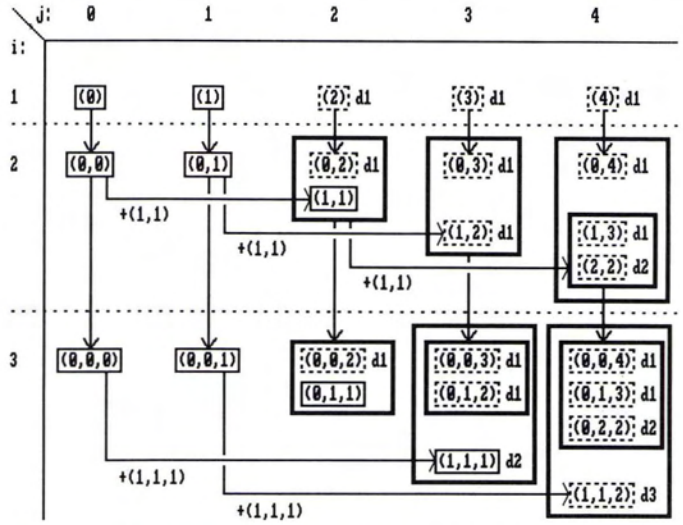

FIG. 3. The combinations ($c(i.j)$) for $i \leq 3$ and $j \leq 4$. (Let 1 be the maximum density: the ($c(i.j)$) which must be deleted are marked in the analogous way as in Figure 2).

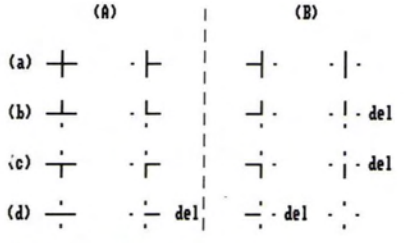

FIG. 5. Possible L/O-occupations of the HLP at position i, of the new HLP at position $i+1$ and the new VLP after the addition of two pixels on the right of line 1 and line 2. The new HLP is occupied by "L" in case (A), by "0" in case (B). (a) - (d) mark the cases of the occupations of the new VLP. Unallowed occupations are marked by "del".

where $h1_{i,x,y}$ resp. $h0_{i,x,y}$ are the numbers of all L/O-occupations in which the ith HLP is occupied by L resp. O (horizontal line resp. dot in Figure 5). We reduce the matrix $\mathbf{M}(i)$ in the same way to $\mathbf{M1}(i) + \mathbf{M0}(i)$.

Step 4: On the right of line 1 and line 2 we add one pixel and, therefore, an ith VLP in each line and a $(i+1)$st HLP. So $\mathbf{M}(i)$ is extended to $\mathbf{M}(i+1)$. These new line positions can be occupied by L or by O (vertical line or dot in Figure. 5). Figure 5 shows the allowed L/O-occupations of the three new added line elements and how to determine $h1_{i+1,x,y}$ and $h0_{i+1,x,y}$:

$$
\begin{aligned}
&\text{(A) (a):} && h1_{i+1,x,y} && = h1_{i,x,y} + h0_{i,x,y}\\
&\text{(B) (a):} && h0_{i+1,x,y} && = h1_{i,x,y} + h0_{i,x,y}\\
&\text{(A) (b):} && h1_{i+1,x+2^{i-1},y} && = h1_{i,x,y} + h0_{i,x,y}\\
&\text{(B) (b):} && h0_{i+1,x+2^{i-1},y} && = h1_{i,x,y}\\
&\text{(A) (c):} && h1_{i+1,x,y+2^{i-1}} && = h1_{i,x,y} + h0_{i,x,y}\\
&\text{(B) (c):} && h0_{i+1,x,y+2^{i-1}} && = h1_{i,x,y}\\
&\text{(A) (d):} && h1_{i+1,x+2^{i-1},y+2^{i-1}} && = h1_{i,x,y}\\
&\text{(B) (d):} && h0_{i+1,x+2^{i-1},y+2^{i-1}} && = h0_{i,x,y}
\end{aligned}
$$

So we have for the matrix $\mathbf{M}(i+1)$:

$$
\begin{bmatrix}
(\mathbf{M1}(i)+\mathbf{M0}(i))+(\mathbf{M1}(i)+\mathbf{M0}(i)) & (\mathbf{M1}(i)+\mathbf{M0}(i))+\mathbf{M1}(i)\\
(\mathbf{M1}(i)+\mathbf{M0}(i)+\mathbf{M1}(i) & \mathbf{M1}(i) + \mathbf{M0}(i)
\end{bmatrix}
$$

Step 5: We add a third line. On each position of $\mathbf{M}_{i+1}$ we have also all L/O-occupations of the HLP between line 2 and line 3 which are possible. We define a vector $(\mathbf{K}(2,i+1,x))$. Each coordinate of it marks the number of those possibilities for the L/O-occupations of the line elements in the line 1/line 2 - rectangle for which the L/O-occupation of the VLP in line 2 belongs to the row x of the matrix $\mathbf{M}(i+1)$. We write $(\mathbf{K}(2,i+1,y))$ for $(\mathbf{K}(2,i+1,x))^T$. We have $(\mathbf{K}(1,i,y)) = (1, \ldots, 1)$, and Figure 6 shows that

$(\mathbf{K}(3,3,y)) = \mathbf{M}(3) \times (\mathbf{K}(2,3,y))$

and $\mathbf{K}(3,3)$ is the sum of all coordinates of $(\mathbf{K}(3,3,y))$, $y = 1, \ldots, 2^2$. In an analogous way we find

$$
\begin{aligned}
(\mathbf{K}(3,i+1,y) &= \mathbf{M}(i+1) \times (\mathbf{K}(2,i+1,y))\\
(\mathbf{K}(r+1,i+1,y)), &= \mathbf{M}(i+1) \times (\mathbf{K}(r,i+1,y))\ r>2,
\end{aligned}
$$

and $\mathbf{K}(i+1,i+1)$ as the sum of all coordinates of the vector $(\mathbf{K}(i+1,i+1))$.

(3) *OECL and CWC not allowed:*

$n = 3$: There are $NA_3 = \mathbf{K}(3,3) - 8$ allowed contour patterns (8 = number of all CWC (Figure 1b)).

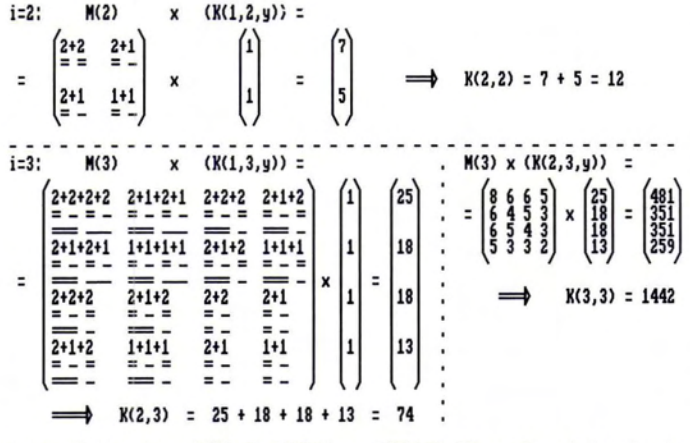

FIG. 6. Calculation of $\mathbf{K}(2,2)$, $\mathbf{K}(2,3)$, and $\mathbf{K}(3,3)$. The values belonging to $\mathbf{M1}(i)$ are marked by =, those belonging to $\mathbf{M0}(i)$ are marked by −.

$n > 3$: For the number NA_n of allowed contour patterns only a low barrier value can be estimated: The CWC with the least number of pixels is that in Figure 1b with eight line positions inside the circle. We have 2^8 possibilities of L/O-occupations of which eight belong to a CWC. Furthermore, we have the possibility of deleting the contours around the pixel (2;2). Thus, $8/(2^8+1) = 1/33$ of all possible L/O-occupations belong to a CWC. If the CWC has $8+h$ pixels, $(8+h)/(2^{8+h}+1) < 1/33$ of all L/O-occupations belong to a CWC. For m positions there are 2^m possibilities for occupancy by a CWC as in Figure 1b or not and 2^m-1 possibilities of having at least one CWC. But there are 33 possibilities of having no CWC at any position. Therefore, the share of CWC is less than $(2^m-1)/33^m$. Because this term is less than 2/33, we have

$$
\begin{aligned}
NA_n/\mathbf{K}(n,n) &> 31/33\\
\geq ld(\mathbf{K}(n,n) - ld(NA_n) &< ld(33/31)) < 0.0902.
\end{aligned}
$$

So the values of $ld(NA_n)$ are located so little below the line "contour 2" in Figure 8 that they cannot be marked. The lines "contour 1" and "contour 2" in Figure 8 are junction lines of the values calculated for a square arrangement of the pixels. For rectangles, we obtain values beneath these lines but not beneath the line "texture," because for a texture base pattern CWC is impossible.

TEXTURES

(1) The pixels of a texture base pattern can only be "black" (B) or "white" (W). For n pixels $P_1, \ldots, P_n$, we have 2^n permutations and $n+1$ combinations of (B) and (W). For $P_1, \ldots, P_n \rightarrow P$, the pixel P can only be (B) or (W) so that there are only $2^n/2 = 2^{n-1}$ permutations and $\text{int}((n+1)/2)$ combinations of (B) (or (W), if P is (B) (or (W)).

(2) We replace "W" by "bright" and "B" by "dark." The density values of the bright (dark) elements belong to the half of the lower (higher) density values. For a total density range s, the number of possibilities for $P_1, \ldots, P_n \rightarrow P$, P dark (bright), is equal to $NP_{s/2,n,d}$ which is the number of equidensities of range $s/2$ formed after (a) the scale reduction.

ILLUSTRATION OF THE MAXIMUM INFORMATION LOSS

The loss of information for $P_1, \ldots, P_n$ can be read in Figures 7 and 8 for different values of n. The number below the horizontal axis marks the number n. For each n there is a group of columns in which the position of each column marks a certain density d of the pixel P; the low densities are on the left of each column group, the high densities on the right. The length of a column is equal to the dual logarithm ld of NP, NC, or N which indicates the loss of information measured by information units.

CONCLUSIONS

(1) The numbers NP, NC, and N (Figures 7 and 8) are a measure of the value of the three information categories and are inversely proportional to their stability. Knowledge about the value of information categories is important, if images with different spatial and radiometric resolution showing the same area of the Earth's surface are compared or MSS-channels of different spatial and radiometric resolution are combined.

(2) If every m neighboring density levels $d_{j1}, \ldots, d_{jm}$ are combined to one equidensity, there are m possibilities that one pixel P_i which belongs to the equidensity E_j has a density value inside the range of the equidensity E_j; for n pixels, there are m^n possibilities. If the equidensities are formed before (b) $P_1, \ldots, P_n \rightarrow P$, there are $m^n * NP_{s_j,n,Ej}$ permutations, if the equidensities are formed after (a) $P_1, \ldots, P_n \rightarrow P$, there are $NP_{s,n,d_{j1}} + \ldots + NP_{s,n,d_{jm}}$ permutations for the density values of $P_1, \ldots, P_n$. Figure 9 shows that the loss of total image information outside the center of the

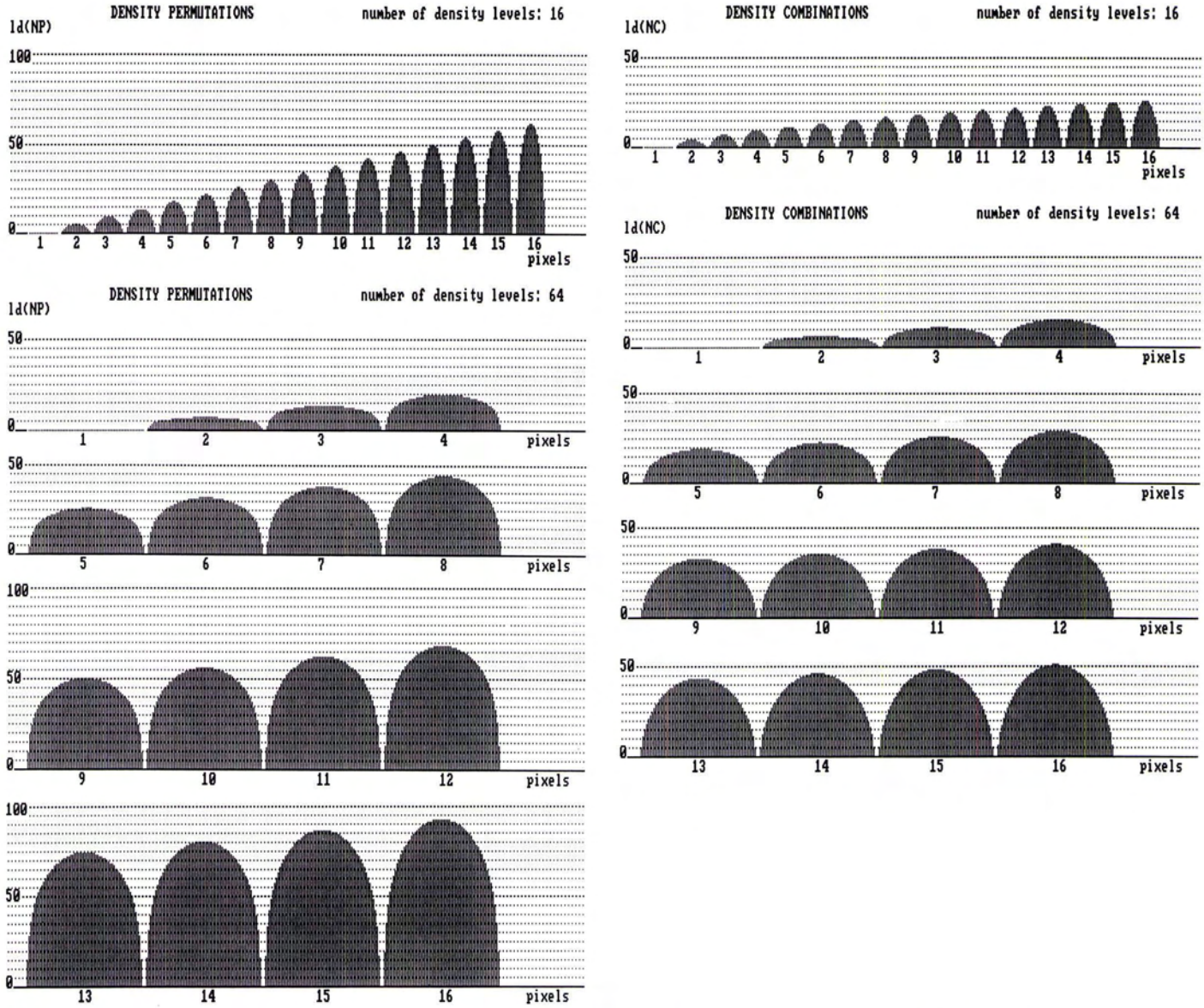

FIG. 7. Dual logarithm ld *d* of the number NP of permutations and the number NC of combinations of the density values of *n* pixels which are united to one pixel (P_1, ..., $P_n \rightarrow P$) with the density d.

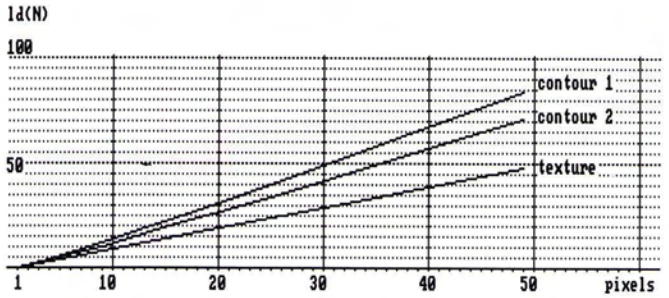

FIG. 8. Dual logarithm of the number
– of possible L/O-occupations of line elements inside a square of *n* pixels (contour 1: OECL allowed, contour 2: OECL unallowed, CWC allowed)
– of possible permutations of *n* black-and-white pixels (texture elements), if P_1, ..., $P_n \rightarrow P$ and *P* white respectively black.

density range is smaller for (b) than for (a). Recording of the Earth's surface by remote sensing systems with lower spatial and higher radiometric resolution causes, therefore, greater loss of information than recording by systems with higher spatial and lower radiometric resolution.

(3) The loss of information is generally much smaller for contours than for the pure density information (density combinations) if the scale reduction is low. This, however, is not valid for low and high density values. If the density range is small, low and high density values have an important share in the total density range (Figures 7 and 8). In this case, automatic systems are superior to the human visual system in analyzing the more stable category of image information. This means a certain "intensification effect" for the application of automatic systems. The reverse is true for the center of the density range and for most of the values of great density ranges. Then the visual system is superior to automatic systems in analyzing the more stable information. This means a certain "intensification effect" for visual image analysis. For higher scale reduction the

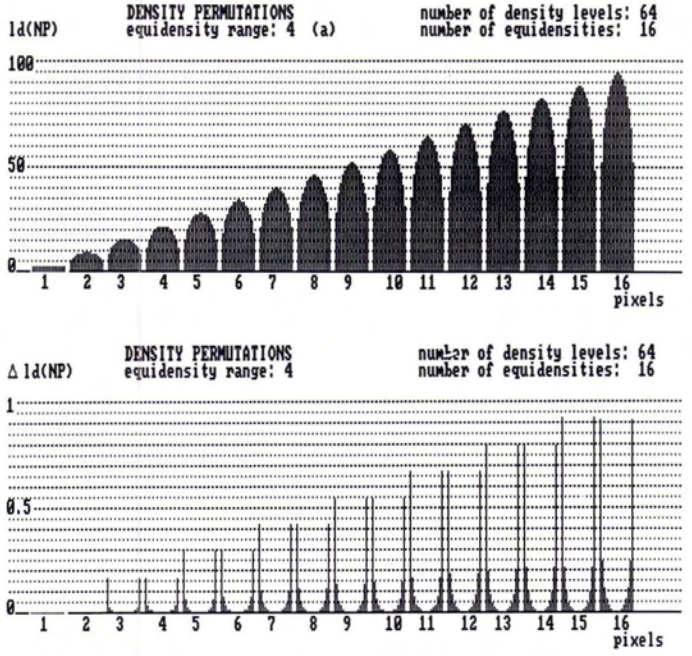

FIG. 9. Above: Dual logarithm of the number of possible density permutations for $P_1, ..., P_n$, where the equidensities are formed after (a) $P_1, ..., P_n \rightarrow P$. Each column represents an equidensity to which P can belong. Below: Difference $ld(NP)(a) - ld(NP)(b)$, where: (a): "equidensities formed after $P_1, ..., P_n \rightarrow P$", (b): "equidensities formed before $P_1, ..., P_n \rightarrow P$". (There is no continuous increasing of the column groups for increasing n because of the differences of the algorithms of calculating NP for even and odd values of n).

loss of pure contour information is the lowest of all information categories so that there is an "intensificatin effect" for the applicatin of automatic systems.

(4) The stability of the full texture information (two equidensities) corresponds to the stability of total image information. More important for analysis of textures, however, are shape and arrangement of pattern elements. Those are the characteristic features of the texture base pattern, the most stable information category for lower degrees of scale reduction (Figure 8) a little less stable than pure density information else. Therefore, the development of automatic systems for texture analysis is particularly worthwhile. The ability of synoptic image perception by the visual system and the ability of recording textural differences which are not perceptible visually by automatic systems can complement one another in an optimal way.

REFERENCES

Gilchrist, A.L., 1986. Die Wahrnehmung schwarzer und weißer Flächen. *Wahrnehmung und visuelles System.* (M. Ritter, editor). Vlg. Spektrum der Wissenschaft, Heidelberg.

Gonzales, R.C., and P. Wintz, 1987. *Digital Image Processing,* Addison-Wesley Publ. Company, Reading, Mass.

Goulden, I.P., and D.M. Jackson, 1983. *Combinatorial Enumeration.* John Wiley & Sons, New York, Chichester, Brisbane, Toronto, Singapore.

Haralick, R.M., 1978. Statistical and Structural Approach to Texture. *Proceedings of the ISP+IUFRO Symposium,* Freiburg, FRG, Vol. I, pp. 379–431.

Halder, H.-R., and W. Heise, 1976. *Einführung in die Kombinatorik.* Carl Hanser Vlg., Mnchen, Wien.

Julesz, B., 1987. Texturwahrnehmung. *Wahrnehmung und Visuelles System* (M. Ritter, editor). Vlg. Spektrum der Wissenschaft, Heidelberg.

Lipkin, B.S., and A. Rosenfeld, 1970. *Picture Processing and Psychopictorics.* Academic Press, New York, London.

Lowell, K.E., 1990. Difference between Ecological Land Type Maps Produced Using GIS or Manual Cartographic Method. *Photogrammetric Engineering & Remote Sensing,* Vol. 56, No. 2, pp. 169–173.

Piaget, J., and B. Inhelder, 1966. *L'Image mentale chez L'Enfant.* Presses Universitaire de France, Paris.

Wieczorek, U., 1982. *Methodische Untersuchungen zur Analyse der Wattmorphologie aus Luftbildern mit Hilfe eines Verfahrens der digitalen Bildstrukturanalyse.* Münchener Geographische Abhandlungen, Bd. 27.

(Received 13 June 1991; accepted 27 December 1991; revised 26 February 1992)

LIST OF "LOST" CERTIFIED PHOTOGRAMMETRISTS

We no longer have valid addresses for the following Certified Photogrammetrists. If you know the whereabouts of any of the persons on this list, please contact ASPRS headquarters so we can update their records and keep them informed of all the changes in the Certification Program. Thank you.

Dewayne Blackburn
Albert Brown
Eugene Caudell
Robert Denny
Leo Ferran
Robert Fuoco
Franek Gajdeczka
George Glaser
William Grehn, Jr.
David Gustafson
Elwood Haynes
F.A. Hildebrand, Jr.
James Hogan
William Janssen
Lawrence Johnson
Spero Kapelas
Francisco Milande
Harry J. Miller
Marinus Moojen
Gene A. Pearl
Joe Pinello
Sherman Rosen
Lane Schultz
Keith Syrett
William Thomasset
Conrad Toledo
Robert Tracy
Lawrence Watson
Tad Wojenka